Available online at www.sciencedirect.com
ScienceDirect
Applied Surface Science 254 (2008) 2866–2870
applied surface science
www.elsevier.com/locate/apsusc

Auger electron spectroscopic study of CO_2 adsorption on Zircaloy-4 surfaces

N. Stojilovic [1], N. Farkas [2], R.D. Ramsier *

The Institute for Teaching and Learning and The Departments of Physics and Chemistry, The University of Akron, Akron, OH 44325-6236, USA

Received 8 May 2007; accepted 13 October 2007
Available online 22 October 2007

Abstract

We investigate the adsorption of CO_2 onto Zircaloy-4 (Zry-4) surfaces at 150, 300 and 600 K using Auger electron spectroscopy (AES). Following CO_2 adsorption at 150 K the graphitic form of carbon is detected, whereas upon chemisorption at 300 and 600 K we detect the carbidic phase. As the adsorption temperature is increased, the carbon Auger signal increases, whereas the oxygen signal decreases. Adsorption at all three temperatures results in a shift of the Zr Auger features, indicating surface oxidation. The effect of adsorbed CO_2 on the Zr(MVV) and Zr(MNV) transitions depends on adsorption temperature and is less pronounced at higher temperatures. On the other hand, changes in the Zr(MNN) feature are similar for all three adsorption temperatures. The changes in the Zr Auger peak shapes and positions are attributed to oxygen from dissociated CO_2, with the differences observed at various temperatures indicative of the diffusion of oxygen into the subsurface region.

Keywords: Zry-4; CO_2; AES; Carbidic carbon; Graphitic carbon

1. Introduction

Unlike CO, which is one of the most frequently studied adsorbates [1], CO_2 has received little attention in the surface science literature, probably due to its thermodynamic stability. However, after discovery that CO_2 was a crucial reactant in methanol synthesis, interest in surface chemistry of this adsorbate grew [2]. From previous work on the interaction between carbon dioxide and metal surfaces it is known that CO_2 dissociates into chemisorbed CO and O on atomically clean Fe, Ni, Re and Rh, whereas on Ag, Os, Pd and Pt it only physisorbs with no evidence of chemisorption (see reference [2] and references therein). In a study of high-temperature Zr ribbons [3], the following reaction is reported to occur at high temperatures:

$$Zr + 2CO_2(g) \rightarrow ZrO_2 + 2CO(g). \quad (1)$$

Since CO_2 is expected to dissociate on zirconium surfaces upon adsorption, it is also relevant to mention former studies of CO adsorption on these surfaces. It was reported that carbon monoxide dissociates at room temperature [4,5] and that carbon resides beneath the oxide layer [5]. Annealing Zr surfaces in the presence of adsorbates resulted in diffusion of the resulting dissociation fragments into the bulk. For example, over a range of temperatures Foord et al. [4] determined the diffusion coefficients for oxygen and carbon to be $D(O) = 7.4 \times 10^{-16} \exp(-50{,}400/RT)$ m^2/s and $D(C) = 3.6 \times 10^{-16} \exp(-64{,}000/RT)$ m^2/s, respectively, where R is the gas constant and T the absolute temperature. Note that oxygen diffuses into the bulk faster than carbon. It was proposed in the same study that upon heating C forms a carbide [5], consistent with what we observed for the C_6H_6/Zr(0 0 0 1) system [6].

Our group investigated the interaction between hydrocarbons (C_6H_6 and C_6H_{12}) and Zr(0 0 0 1) surfaces [6–9]. We found that after initial dissociation of adsorbates on reactive Zr surfaces, the C-modified Zr surfaces exhibit strong interaction with these hydrocarbons, as indicated by molecular desorption at unexpectedly high temperatures. The exceptional stability of organic species on metal carbides has been reported by other groups as well. For example, in studying benzene layers on

* Corresponding author. Tel.: +330 972 8584; fax: +330 972 8699.
E-mail address: rex@uakron.edu (R.D. Ramsier).
[1] Present address: Department of Applied Physics and Applied Mathematics, Columbia University, New York, NY 10027, USA.
[2] Present address: Precision Engineering Division, National Institute of Standards and Technology, Gaithersburg, MD 20899-8212, USA.

0169-4332/$ – see front matter © 2007 Elsevier B.V. All rights reserved.
doi:10.1016/j.apsusc.2007.10.028

W(1 1 0), Whitten and Gomer reported C–H bonds at temperatures as high as 1400 K [10], whereas the McBreen group reported extreme stability of alkylidene groups on β-Mo_2C under vacuum conditions [11]. In our C_6H_6/Zr(0 0 0 1) experiments we detected C(KLL) Auger line shapes that resemble carbidic and graphitic forms of carbon, and showed that the dominant phase depends on hydrocarbon exposure and sample temperature [6]. In the present work we investigate how the C(KLL) line profiles change with CO_2 exposure at various temperatures, where carbon competes with oxygen rather than with hydrogen for near-surface sites.

Zircaloy-4 (Zry-4) was chosen for this study since much is known about the oxidation kinetics of zirconium alloys used for nuclear applications, but little is known about the oxidation process in the presence of near-surface carbon. Zr has one of the smallest neutron absorption cross-sections among the metals, which is essential for neutron economy during electrical power production. Zr also exhibits excellent corrosion resistance at high temperatures; thus, these alloys are used as structural materials in nuclear reactors. Due to the requirement for materials with high neutron transparency, the content of other elements such as Sn and Fe in Zry-4 is kept very low (total below 2%). It is important to note that the oxide films formed on the surface of zirconium alloys play an essential role in preventing corrosion and hydrogen embrittlement. Here we probe the formation of surface oxides on Zry-4 in the presence of near-surface carbon.

2. Experimental details

Experiments were performed under ultra-high vacuum (UHV) conditions at a pressure of 5×10^{-10} Torr or lower. Detailed descriptions of our UHV chamber and its pumping system are presented elsewhere [12]. Briefly, during experiments an ion getter pump was used, and during 2 keV Ar-ion sputtering or pumping of the gas-handling system a turbomolecular pump was employed. Gas exposures were performed with a translatable line-of-sight molecular beam doser, whose design is presented elsewhere [6]. Exposure to carbon dioxide is expressed in number of gas molecules per unit surface area (cm^2). The CO_2 was purchased from Matheson and had a purity of 99.99%. For Auger electron spectroscopy (AES) experiments, a retarding field Auger system, operating at 3 keV, was used.

The Zry-4 sample has surface area of 0.53 cm^2 and a thickness of 2 mm. The elemental composition of Zry-4 in wt % is nominally 1.2–1.4% Sn, 0.2% Fe, 0.2% Cr + O + Si, and the balance Zr. DC heating was performed via tantalum wires that are spot-welded to the sample, whereas cooling was carried out using a copper braid connected to a liquid-nitrogen cold finger. The sample temperature was measured using type-E (Chromel-Constantan) thermocouples spot-welded to its sides. Cleaning of the sample was accomplished by sputtering cycles followed by annealing to about 920 K which reduces the amount of carbon and oxygen contaminants significantly. After cleaning, the AES peak-to-peak height ratios are typically C(KLL)/Zr(MNN) < 0.10 and O(KLL)/Zr(MNN) < 0.10. We have recently shown that short annealing to 920 K does not result in significant sulfur segregation to the near-surface region of Zry-4 [13], and our cleaning procedure reduces the [Zr(MNV) + S(LMM)]/Zr(MNN) ratio to 1.3, which, according to previous studies, corresponds to sulfur-free Zr surfaces [4,14,15].

3. Results and discussion

Fig. 1 shows how the C(KLL)/Zr(MNN) (filled points) and O(KLL)/Zr(MNN) (hollow points) Auger peak-to-peak height

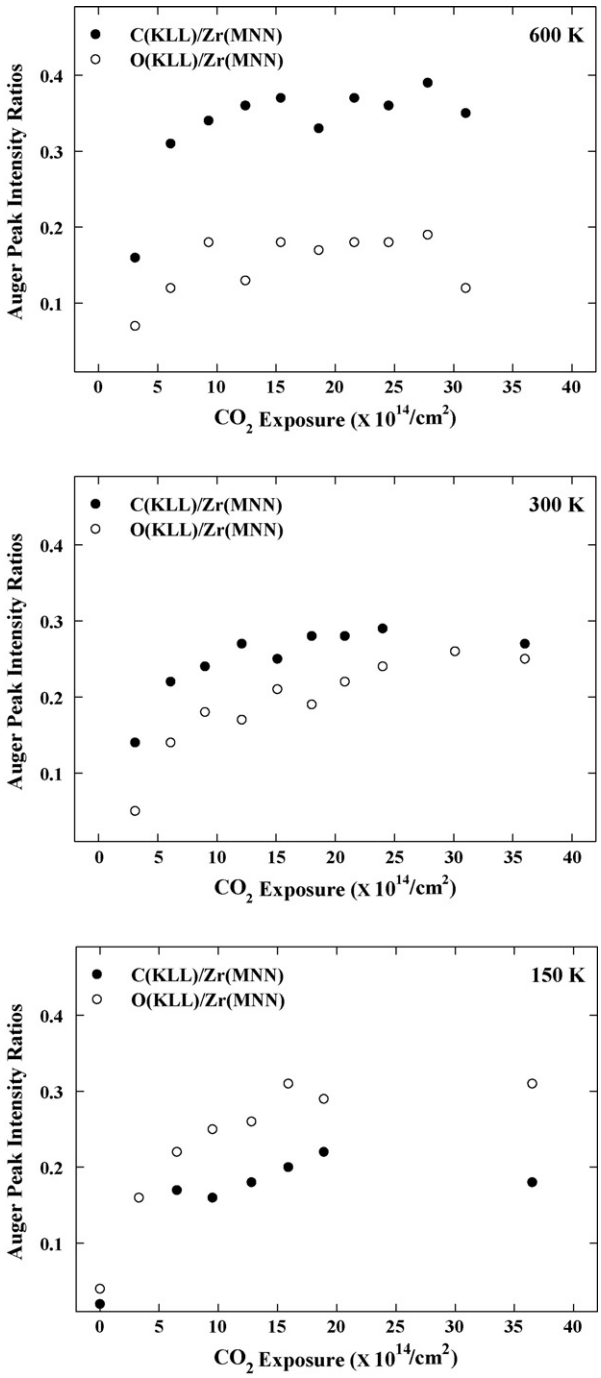

Fig. 1. C(KLL)/Zr(MNN) (filled points) and O(KLL)/Zr(MNN) (hollow points) Auger peak-to-peak height ratios versus CO_2 exposure at 150, 300 and 600 K.

ratios change with CO_2 exposure at three different sample temperatures. Following CO_2 adsorption at 150 K (bottom panel) the O(KLL) signal is greater than that of carbon. At 300 K (middle panel) the C(KLL) signal, consistent with the work on CO/Zr [4], becomes greater than that of the O(KLL). The trend continues and at 600 K (upper panel) the C(KLL) signal becomes even larger with the oxygen signal becoming smaller. We normalize the C and O AES features with respect to Zr(MNN) which is, as will be discussed later, not significantly affected by the adsorbed species.

The fact that the oxygen Auger signal is reduced at higher temperatures, in particular at 600 K, can be attributed to the greater diffusion coefficient as compared to that of carbon [4]. Also, it is known that atomic oxygen favors subsurface sites, especially at higher temperatures [16]. In a study of oxygen adsorption on zirconium single crystals it was reported that at 90 K 70–75% of oxygen absorbs directly into the subsurface region, whereas upon adsorption at 473 K oxygen entirely resides subsurface and is stable against further diffusion into the bulk up to about 573 K [16]. In our experiments here, there is a temperature-dependent competition between C and O species for surface and subsurface sites.

Since Auger transitions involve bonding electrons, change in a line shape may accompany changes in bonding and reflect different chemical environments. For example, the carbon Auger feature may be used to distinguish carbidic from graphitic phases [10]. Fig. 2 shows the line shape of the C(KLL) feature following Zry-4 exposure to 5×10^{14} CO_2/cm^2 at 150, 300 and 600 K. At 150 K the carbon Auger peak resembles that of graphitic carbon [10]. On the other hand, Auger signatures on the low kinetic energy side upon CO_2 chemisorption at 300 and 600 K are characteristic of the carbidic phase, where the term carbidic originates from the resemblance of the C(KLL) line shape to the corresponding bulk metal carbide.

In the data of Fig. 2, at 300 and 600 K carbon has a similar line shape and we can make direct comparison of the C(KLL) signal intensities. At the low exposures of Fig. 2, the carbon features are similar in size. However, as seen in Fig. 1, larger exposures at higher temperatures result in increased C(KLL) relative intensities. This is a result of faster oxygen diffusion into the subsurface region, especially at 600 K, that leaves carbon dominant at the surface.

It is known that these two carbon phases have significantly different electronic structures and reactivity [18]. Feibelman proposed models for carbidic and graphitic carbon overlayers on Ru(0 0 0 1) and an explanation as to why carbidic carbon is reactive while the graphitic phase is not [18]. He concluded that the C($2p_z$) (the z axis pointing along surface normal) orbital is not involved in bonding of carbon to the surface and has a density of states peak near the Fermi energy, and is probably the dangling bond responsible for the reactivity of the carbide. In the graphitic phase, p_z orbitals interact via π bonds with each other, and thus are not able to engage in additional interactions. Carbidic carbon is observed in our case at 300 and 600 K, consistent with other work on early transition metals [19]. We should note that it is possible that both carbon phases coexist on the surface, as observed in an AES study of CO on Ni(1 0 0) [20]. However,

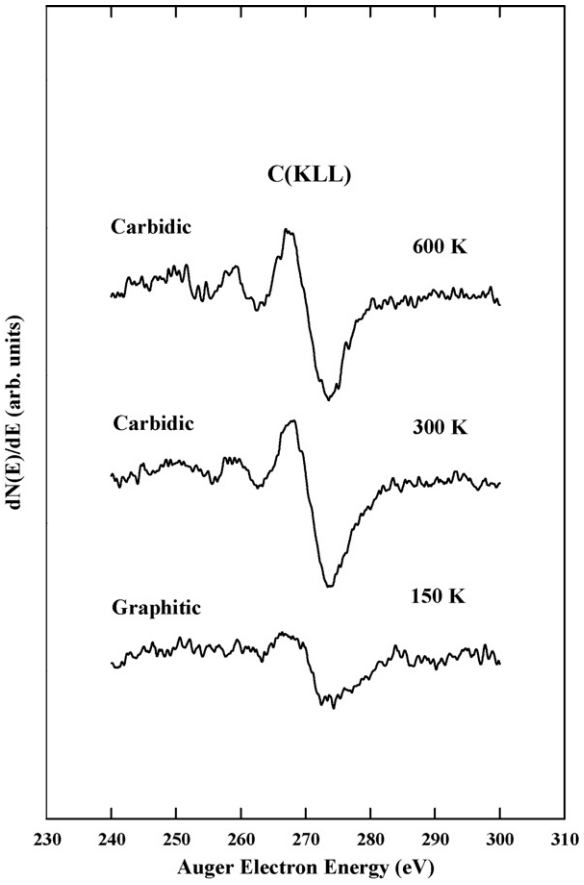

Fig. 2. Derivative mode Auger electron spectra showing the C(KLL) transition as a function of adsorption temperature. In all three cases an exposure to CO_2 of $5 \times 10^{14}/cm^2$ is used. Upon CO_2 adsorption at 150 K the line shape resembles that of graphitic carbon, whereas in the 300 and 600 K cases the carbidic-like phase dominates.

dominance of each phase at different temperatures can be inferred from Fig. 2.

Changes in the oxidation state of Zr indicate the formation of surface oxide following dissociation of CO_2. Potential fragments are CO and O with the possibility of further CO dissociation as observed in a study of CO interaction with Zr [4,5]. Since we are using AES, it is difficult to completely rule out electron-beam effects on adsorbed species. Hooker and Grant reported significant electron-beam effects on the O(KLL) and C(KLL) Auger features within several minutes of irradiation of CO/Ni [17]. They reported that the electron beam decomposes CO into surface carbide and oxide. In the same study [17] it was reported that oxygen concentration decreased faster under electron bombardment than carbon.

Since Zr is well known for binding adsorbed atoms beneath the outermost surface layer, the effects of electron-beam damage are expected to be reduced. In addition, our various temperature CO_2/Zry-4 experiments were conducted under identical electron beam exposure conditions, so if electron-beam effects are present these should be similar in all three cases. Observed differences in our AES data for different CO_2 adsorption temperatures are, therefore, not attributed to electron-beam effects.

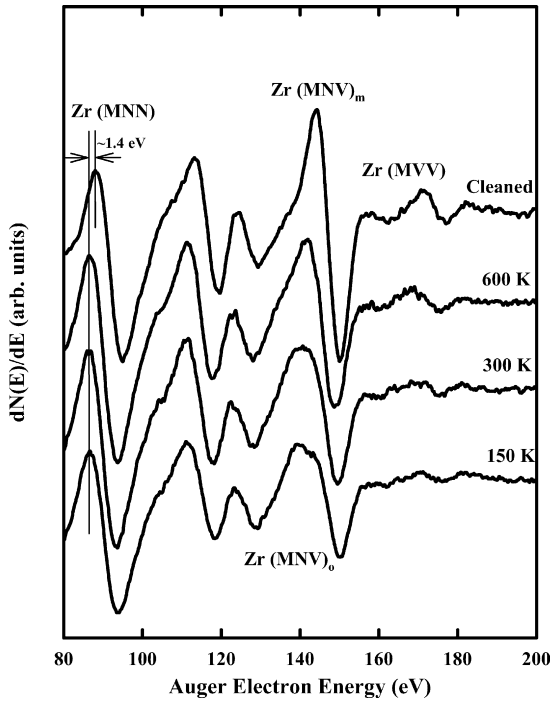

Fig. 3. Derivative mode Auger electron spectra showing zirconium Auger transitions after exposure to CO_2 (40×10^{14}/cm^2) at 150, 300, and 600 K. The vertical line on the Zr(MNN) transition is inserted to stress the shift toward lower energies that directly reveals surface oxidation. Regardless of adsorption temperature and exposure in the 5–40×10^{14}/cm^2 interval, the Zr(MNN) feature shifts by about 1.4 eV. Following CO_2 adsorption at 150 K the $Zr(MNV)_o$ (oxide) feature appears. The strongest effect on the Zr(MVV) transition is observed at 150 K and is reduced as the adsorption temperature is increased.

Fig. 3 shows the Zr AES transitions after exposure of Zry-4 to 40×10^{14}/cm^2 of CO_2 at 150, 300, and 600 K. The effect of adsorbed species on the spectra is reflected in the peak shape changes and reduction of Auger electron signal intensities. Here, we will concentrate on the Zr(MVV), Zr(MNV) and Zr(MNN) features. It is evident from the figure that different transitions are affected in various ways. The greatest effect, as expected, is observed on the Zr(MVV) transition involving two valence electrons. This peak is most affected at 150 K and becomes less affected as the adsorption temperature is increased to 300 and 600 K.

The $Zr(MNV)_m$ (metallic) peak is reduced and shifted toward lower energy by 2.2, 3.6 and 5 eV at 600, 300 and 150 K, respectively. This shift can be thought of as the appearance of a new oxide feature, $Zr(MNV)_o$ (oxide) [21,22], which becomes visible in the spectrum after 150 K CO_2 adsorption where the strongest oxygen signal is observed (see Fig. 1). It is interesting to note that this feature, $Zr(MNV)_o$, was much more visible after Zry-4 exposure to water [22], and oxygen [23] in our previous studies. It is likely, based on the shifts in Zr Auger features, that following adsorption of CO_2 on Zry-4 the oxidation state of Zr is less than +4. Thus, reaction (1), as reported in an earlier study of Zr [3], does not seem to apply under our experimental conditions.

The absence of a fully oxidized surface layer in our case is attributed to the presence of carbon that probably still interacts with oxygen, thus reducing oxygen's ability to attract Zr electrons. The change in the Zr(MNN) peak profile is much smaller than in the other two transitions discussed above. Within experimental uncertainty, there is essentially no change in the actual signal intensity of this feature, except maybe following CO_2 adsorption at 150 K. The shift of about 1.4 ($\pm$0.2) eV in the Zr(MNN) feature is observed at all three temperatures as indicated in the figure by the inserted vertical lines. The same shift is observed (not indicated) on the high kinetic energy side of the same Zr(MNN) peak. Even though little change is observed on the Zr(MNN) transition at these three temperatures, from the features involving valence electrons we see that the effect of adsorbed species is strongest at 150 K when the O(KLL) signal is largest (Fig. 1).

Since our earlier experiments on C_6H_6/Zr(0 0 0 1) showed no shift in the Zr Auger features that would indicate surface oxidation [6], we propose that the shift in Zr features toward lower energies reflects electron donation from zirconium to oxygen. Our annealing experiments (data not shown here) support the claim that these shifts in Zr features are induced by the presence of oxygen. This is consistent with the fact that when the oxygen Auger signal is the weakest (600 K adsorption), there are the smallest effects on the transitions involving valence electrons, Zr(MVV) and Zr(MNV), with respect to cleaned surface spectra.

4. Concluding remarks

Upon exposure of Zry-4 surfaces to CO_2, AES reveals two states of adsorbed carbon that resemble carbidic and graphitic phases, depending on adsorption temperature. After CO_2 adsorption at 150 K, the graphitic phase is dominant, whereas upon 300 and 600 K adsorption, the line shape of the C(KLL) resembles that of carbidic carbon. The oxidation of the near-surface region is evident from the shift in the Zr Auger features toward lower energies, reflecting the electropositive nature of zirconium. CO_2 adsorption at all three temperatures results in a shift of the Zr(MNN) transition by about 1.4 $\pm$ 0.2 eV, whereas Zr(MNV) features shift and change shape. We attribute the changes in the Auger peak positions to the presence of oxygen as no such shift is observed for C_6H_6/Zr(0 0 0 1) [6]. Additional evidence for the Zr peak shifts being induced by oxygen is the fact that removal of the oxide film is accompanied by oxygen, not carbon, dissolution into the bulk. AES signal intensities of the C(KLL) and O(KLL) features are a function of adsorption temperature. At 150 K the O(KLL) signal is stronger than that of C(KLL), and as the adsorption temperature is increased, the C(KLL) signal becomes dominant indicating that there is a competition among dissociation fragments for the near-surface sites of the alloy.

Acknowledgement

We thank Wah Chang for providing the Zry-4 material used in this study.

References

[1] J.T. Yates Jr., Surf. Sci. 299/300 (1994) 731.
[2] H.-J. Freund, M.W. Roberts, Surf. Sci. Rep. 25 (1996) 225.
[3] C.M. Quinn, M.W. Roberts, Trans. Faraday Soc. 59 (1963) 985.
[4] J.S. Foord, P.J. Goddard, R.M. Lambert, Surf. Sci. 94 (1980) 339.
[5] G.B. Hoflund, G.R. Corallo, D.A. Asbury, R.E. Gilbert, J. Vac. Sci. Technol. A 5 (1987) 112.
[6] N. Stojilovic, J.C. Tokash, R.D. Ramsier, Surf. Sci. 565 (2004) 243.
[7] N. Stojilovic, R.D. Ramsier, Solid State Commun. 130 (2004) 623.
[8] N. Stojilovic, R.D. Ramsier, Chem. Phys. Lett. 399 (2004) 53.
[9] N. Stojilovic, J.C. Tokash, S.P. McGinnis, R.D. Ramsier, J. Vac. Sci. Technol. A 23 (2005) 1013.
[10] J.E. Whitten, R. Gomer, Surf. Sci. 347 (1996) 280.
[11] M. Siaj, P.H. McBreen, Science 309 (2005) 588.
[12] Y.C. Kang, M.M. Milovancev, D.A. Clauss, M.A. Lange, R.D. Ramsier, J. Nucl. Mater. 281 (2000) 57.
[13] N. Stojilovic, E.T. Bender, R.D. Ramsier, Appl. Surf. Sci. 252 (2005) 1806.
[14] T.W. Haas, J.T. Grant, G.J. Dooley, Phys. Rev. B 1 (1970) 1449.
[15] P.C. Wong, K.A.R. Mitchell, Can. J. Chem. 64 (1986) 2409.
[16] C.-S. Zhang, B.J. Flinn, I.V. Mitchell, P.R. Norton, Surf. Sci. 245 (1991) 373.
[17] M.P. Hooker, J.T. Grant, Surf. Sci. 55 (1976) 741.
[18] P. Feibelman, Surf. Sci. 103 (1981) L149.
[19] J.G. Chen, M.D. Weisel, Z.M. Liu, J.M. White, J. Am. Chem. Soc. 115 (1993) 8875.
[20] J. Nakamura, H. Hirano, M. Xie, I. Matsuo, T. Yamada, K. Tanaka, Surf. Sci. 222 (1989) L809.
[21] C. Zhang, P.R. Norton, J. Nucl. Mater. 300 (2002) 7.
[22] N. Stojilovic, R.D. Ramsier, Surf. Interf. Anal. 38 (2006) 139.
[23] N. Stojilovic, E.T. Bender, R.D. Ramsier, J. Nucl. Mater. 348 (2006) 79.